The radiative influence of aerosol effects on liquid-phase cumulus clouds based on sensitivity studies with two climate models

Surabi Menon[1] and Leon Rotstayn[2]
[1]Lawrence Berkeley National Laboratory, Berkeley, CA, USA
(smenon@lbl.gov, Tel: 1 510 486 6752, Fax: 1 510 486 5928)
[2]CSIRO Marine and Atmospheric Research, Aspendale, Victoria, Australia
(leon.rotstayn@csiro.au, Tel: 61 2 9239 4542, Fax: 61 2 9239 4444)

Submitted to Climate Dynamics

October 5, 2005

The radiative influence of aerosol effects on liquid-phase cumulus clouds based on sensitivity studies with two climate models

Surabi Menon[1] and Leon Rotstayn[2]
[1]Lawrence Berkeley National Laboratory, Berkeley, CA, USA
[2]CSIRO Marine and Atmospheric Research, Aspendale, Victoria, Australia

Abstract

Aerosol effects on warm (liquid-phase) cumulus cloud systems may have a strong radiative influence via suppression of precipitation in convective systems. A consequence of this suppression of precipitation is increased liquid water available for large-scale stratus clouds, through detrainment, that in turn affect their precipitation efficiency. The nature of this influence on radiation, however, is dependent on both the treatment of convective condensate and the aerosol distribution. Here, we examine these issues with two climate models – CSIRO and GISS, which treat detrained condensate differently. Aerosol-cloud interactions in warm stratus and cumulus clouds (via cloud droplet formation and autoconversion) are treated similarly in both models. The influence of aerosol-cumulus cloud interactions on precipitation and radiation are examined via simulations with present-day and pre-industrial aerosol emissions. Sensitivity tests are also conducted to examine changes to climate due to changes in cumulus cloud droplet number (N_c); the main connection between aerosols and cumulus cloud microphysics. Results indicate that the CSIRO GCM is quite sensitive to changes in aerosol concentrations such that an increase in aerosols increases N_c, cloud cover, total LWP and reduces total precipitation and net cloud radiative forcings. On the other hand, the radiative fluxes in the GISS GCM appear to have minimal changes despite an increase in aerosols and N_c. These differences between the two models --reduced total LWP in the GISS GCM for increased aerosols, opposite to that seen in CSIRO-- appear to be more sensitive to the detrainment of convective condensate, rather than to changes in N_c. If aerosols suppress convective precipitation as noted in some observationally based studies (but not currently treated in most climate models), the consequence of this change in LWP suggests that: (1) the aerosol indirect effect (calculated as changes to net cloud radiative forcing from anthropogenic aerosols) may be higher than previously calculated or (2) lower than previously calculated. Observational constrains on these results are difficult to obtain and hence, until realistic cumulus-scale updrafts are implemented in models, the logic of detraining non-precipitating condensate at appropriate levels based on updrafts and its effects on radiation, will remain an uncertainty.

1. Introduction

Aerosol effects on precipitation formation in both large-scale stratus and cumulus clouds have been observed over the last several years via satellite data (Rosenfeld and Lensky 1998, Rosenfeld and Woodley 2000, Rosenfeld 1999, 2000; Shepherd et al. 2001). Aerosol effects on large-scale stratus clouds studied via several climate models (Lohmann et al. 1999; Ghan et al. 2001; Rotstayn and Lohmann 2002a; Menon et al. 2002; Menon 2004; Takemura et al. 2005;

Lohmann and Feichter 2005) suggest that the suppression of precipitation with increased aerosols can alter the radiative fluxes due to changes in cloud lifetime or liquid water path (LWP). However, observed changes to convective cloud precipitation due to aerosol effects are only now being studied via global climate models (Nober et al. 2003, Menon and Del Genio 2006). Aerosol effects on cumulus clouds, while not radiatively significant, are important dynamically since latent heat released from tropical convection impacts the general circulation in tropical regions (Graf 2004). Precipitation changes in convective systems not only affect the vertical release of latent heat flux but can also shift the droplets that could coalesce to higher levels (Andreae et al. 2004). Since convective systems are linked to large-scale stratiform cloud systems via detrained water and moisture, the overall effects of aerosols on both these cloud systems will provide a useful indicator on the influence of aerosols on precipitation as well as radiation and the sensitivity of schemes that treat these processes.

For convective systems, changes to the water cycle; via precipitation that reduces the amount of condensate in the updrafts, and detrained condensate that form anvil clouds, need to be well characterized to obtain appropriate cloud feedbacks (Del Genio et al. 2005, hereafter DG05). Based on observational analysis, DG05 find that convective and associated cirrus anvil amount depend on large-scale dynamical conditions as well as on the sea-surface temperatures. By suppressing precipitation in convective systems, one may also consider an aerosol influence on these processes, that may increase anvil formation, similar to the 'thermostat hypothesis' (Ramanathan and Collins 1991); except that the increased condensate here is not due to the increase in warming but rather due to the reduction in droplet sizes from the aerosol effect that acts to suppress precipitation. Furthermore, detrained condensate from cumulus clouds increase liquid water available for stratus clouds, thereby influencing LWP as well as precipitation efficiency of these clouds, in addition to the relative humidity profiles that can increase stratus cloud cover. The larger radiative effects usually obtained from changes to stratus cloud systems suggest that the detrained condensate and precipitation processes in cumulus clouds may have a strong indirect influence on the radiative forcing of stratus cloud systems.

We examine aerosol effects on warm cumulus, in addition to their effects on warm stratus via two climate models – the Commonwealth Scientific and Industrial Research Organisation (CSIRO) GCM and the Goddard Institute for Space Studies (GISS) GCM. Here, warm clouds refer to liquid-phase clouds. Changes in precipitation, as well as cloud properties are examined between simulations with present-day (PD) versus pre-industrial (PI) aerosol emissions to understand the role that anthropogenic aerosols play in modifying precipitation and radiation. Several sets of simulations are conducted to quantify the climate effects associated with the coupling between aerosol-cumulus and aerosol-stratus clouds. Sensitivity tests have also been conducted to provide an indication of the sensitivity of precipitation to cloud droplet number concentration (N_c). General features of changes to climate from aerosols are studied between models without accounting for systematic differences between model physics since our focus is mainly on parameterization differences that cause a specific climate response in a model due to an imposed forcing (in this paper we only focus on aerosol effects on warm clouds). Both models however use a similar treatment for calculating N_c and the autoconversion process in warm clouds, which are the main processes linked with aerosols.

2. Model Description and Simulations

The standard features of the CSIRO and GISS GCMs relevant to cloud processes and the GCM in general are described below. The effects of aerosols on warm stratiform clouds in these models are described previously in Rotstayn and Liu (2003, 2005) and Menon et al. (2002, 2003).

The CSIRO GCM is a low-resolution (spectral R21) version of the CSIRO Mk3 GCM described by Gordon et al. (2002; http://www.dar.csiro.au/publications/gordon_2002a.pdf). Aerosol treatments have recently been added, as described by Rotstayn and Lohmann (2002b) for the sulfur cycle, and based on Cooke and Wilson (1996) for carbonaceous aerosols. The model includes a physically based stratiform cloud microphysical scheme (Rotstayn 1997) although the treatment of cloud fractional coverage is simple, being based on an assumed triangular distribution of subgrid moisture (Smith 1990). The CSIRO model's convection scheme (Gregory and Rowntree 1990) uses a single "bulk" cloud model to represent an ensemble of convective elements. In convective clouds, a simple threshold-based scheme is used for warm rain formation, whereby all condensate in excess of a prescribed mixing ratio threshold, q_{min}, is allowed to precipitate. In the standard version of the scheme, information regarding aerosols is assumed to be unavailable, and q_{min} is set to $0.5 \min[1 \text{ g/kg}, q_{sat}]$, where q_{sat} is the saturation mixing ratio at the parcel's temperature and pressure. We modify q_{min} to vary with aerosol concentration as described below. The convective cloud water mixing ratio that is saved for the radiation scheme is taken as the average of the values before and after the release of precipitation. At convective cloud top, all condensate in excess of q_{min} is detrained and is made available to the large-scale cloud scheme, but there is no detrainment of convective condensate below cloud top.

In the GISS GCM the prognostic treatment of cloud water include sources from large-scale convergence and cumulus detrainment as well as sinks due to autconversion, accretion, evaporation, and cloud top entrainment, as well as precipitation enhancement due to the seeder-feeder effect (Del Genio et al. 1996). Stratiform cloud cover is diagnosed as a function of relative humidity and stability and subgrid vertical cloud fraction is accounted for. For moist convection, a quasi-equilibrium cloud base closure with entraining and non-entraining updrafts and a cumulus-scale downdraft is used. In the older version of the GISS GCM all condensate was converted to precipitation below freezing levels and above freezing, 50% was detrained (Del Genio and Yao 1993). In the new version of the GISS GCM (Hansen et al. 2005; Schmidt et al. 2005) used in this study, the partioning of convective condensate between precipitation and detrainment into anvil clouds is based on a microphysics scheme that uses a Marshall-Palmer distribution for cloud droplets, empirical droplet size - terminal velocity relationships for liquid, graupel, and ice hydrometeors and prescribed cumulus updraft speeds (DG05). This scheme only applies to deep convective clouds, and for shallow convection all condensate is allowed to precipitate. The addition of the cumulus microphysics scheme is an important addition in the newer version of the GISS GCM and the influence of this scheme on cloud feedbacks are discussed in DG05.

We perform several sets of simulations to separate between aerosol-cumulus and aerosol-stratus effects: (1) Exp CON: Aerosol effects on warm cumulus clouds; (2) Exp CON_C: Similar to Exp

CON but using monthly mean two-dimensional N_c distributions from the CSIRO GCM to eliminate the effects of different aerosol burdens– see Section 3.2; (3) Exp CON_S: Similar to Exp CON but including aerosol effects on warm stratiform clouds and the direct aerosol effects (i.e. aerosols are allowed to interact with the radiation scheme). The basic features of the microphysics schemes relevant to processes described in this paper are listed in Table 1. For the autoconversion scheme, for convective clouds, q_{min} is modified so that it is based on a threshold droplet effective radius of 14 μm (Costa et al. 2005). The relation between volume-mean radius r_v and effective radius, r_e is $r_v=r_e/\beta$. Here, β is the spectral shape factor defined as a function of the relative dispersion, γ, the ratio of the standard deviation to the mean radius of the droplet number size distribution (Liu and Daum 2000). Then q_{min} is obtained as a function of the critical volume mean radius (r_{vc}) as:

$$q_{\min} = \frac{4\pi\rho_l r_{vc}^3 N_c}{3\rho} \qquad (1)$$

Here, ρ and ρ_l are the density of air and liquid water respectively. This scheme is applied to liquid-phase cumulus clouds in both models. In the CSIRO GCM, no mixed-phase cumulus clouds are allowed, and liquid-phase cumulus clouds are defined as those with temperatures above 258.15K. In the GISS GCM (which includes a mixed-phase category) liquid-phase cumulus clouds are defined as those with temperatures greater than 273.15K. The cumulus microphysics scheme is only applied to deep convective clouds in the GISS GCM, hence aerosol effects on shallow convective precipitation are neglected. However, since shallow convective cloud cover is larger over the oceans than over the continents, where it is underestimated relative to observed surface climatologies; and given that changes in N_c occur more over continents than over oceans, the aerosol effect on shallow convective precipitation may be small for the GISS GCM (Del Genio, Personal Communication). For stratus clouds, both models use similar autoconversion treatments based on Rotstayn and Liu (2005).

N_c in convective clouds is obtained as shown in Table 1 and is based on Segal et al. (2004). Aerosol emissions used in the two models are given in Appendix A. The conversion of aerosol mass predicted by the model to aerosol number are given in Appendix A. N_c for stratiform clouds are based on Gultepe and Isaac (1999) as described in Menon and Del Genio (2006) and Hansen et al. (2005). All runs use climatological mean sea-surface temperatures for present-day conditions and are averaged over five years after a spin-up of one year.

3. Results

Below, we describe results from three sensitivity tests mainly conducted to illustrate changes to precipitation and radiation from aerosol effects on cumulus clouds.

3.1. Sensitivity of cumulus clouds to aerosols: Some of the main differences between the two models may be related to the differences in aerosol fields used in the two models that were generated from different aerosol emission sources. Dust aerosols are not allowed to influence N_c due to considerable uncertainty in the knowledge of their soluble fraction and their anthropogenic component. The sea-salt aerosol burdens do not change appreciably between PD

and PI conditions, and are comparable in both the CSIRO and GISS GCMs (5.52 mg m^{-2} in CSIRO and 5.6 mg m^{-2} in GISS). However, the other aerosols that affect N_c (sulfates, organic matter (OM) and black carbon (BC)) differ between PD and PI conditions, have a large anthropogenic component, and also differ between the models. The lower total burden of these aerosols in the GISS GCM (3.71 and 1.64 mg m^{-2} for PD and PI aerosol emissions, respectively) compared to the CSIRO GCM (7.34 and 2.67 mg m^{-2} for PD and PI aerosol emissions, respectively) is partly due to lower SO_2 and biomass emissions used (Menon and Del Genio 2006); and mainly due to the use of a dissolved species budget that reduces the sulfate produced from clouds since more sulfate is being rained out rather than being returned to the grid box at the end of the model time step as in other chemistry models (Koch et al. 2003). This results in less sulfate aerosol available in cloud water. To compensate for the large differences in anthropogenic aerosol burden between the two models we increase industrial SO_2 (factor of 4) and biomass emissions (factor of 2) in the GISS GCM so that the anthropogenic components are more comparable between the models. We refer to this as Exp CON. Differences between Exp CON and Exp CON_S (standard aerosol emissions) for GISS for PD and PI aerosol emissions indicate that apart from changes to aerosol burdens, the net top of the atmosphere (TOA) radiation and N_c, differences in other diagnostics are less than 5%.

To understand the response of cloud properties to differences in parameterizations used in the two models, we focus on differences for Exp CON for PD versus PI aerosol emissions (sulfur, OM and BC). In Figure 1, vertical profiles of global annual averaged aerosol mass are shown for the two models. We note that in CSIRO high values at the surface decrease exponentially as a function of height, and aerosol mass values are also higher than that of GISS for the surface and lower layers of the atmosphere. The main sources of OM and sulfate for the PI cases are from biomass and volcanic emissions, respectively. Annual average differences between PD and PI simulations are given in Table 2. Since N_c values will be different at different levels, to facilitate a comparison of N_c between the two models, we use the model levels closest to 750 hPa since aerosol mass simulated by the models at this level is comparable, as seen in Fig. 1. Changes between the two models, as shown in Table 2, include: more negative values for the net TOA and net cloud radiative forcing (CRF) mainly due to the larger changes in LWP, total and convective cloud cover for CSIRO. Although the CSIRO values for N_c are larger than those from GISS for the column, changes in N_c (grid-box mean) for CSIRO, as shown in Table 2, are smaller at the level closest to 700 hPa, since the CSIRO aerosol mass is lower at this level. For CSIRO, N_c values for moist convective clouds are largest near the surface, although the lowest levels would generally be below cloud base, and in GISS, values of N_c are highest between 850 to 740 hPa.

Changes in convective precipitation are shown in Fig. 2 for both models and tend to decrease mainly for convective cases since the total precipitation change is offset by a slight increase in stratus precipitation (from moist convective anvils). However, these changes are rather small. Areas of decreases in convective precipitation generally follow areas with an increase in warm moist convective N_c (Fig. 3) in the GISS model. Similar features are also seen in the CSIRO model with adjacent areas tending to show a compensating increase of convective precipitation. Convective precipitation accounts for ~ 82% of the total precipitation in the CSIRO model; whereas in GISS the convective fraction of total precipitation is about 56%. To evaluate the differences between the two models more meaningfully would require global distributions of

precipitation that are difficult to obtain, especially the partitioning between the stratiform and convective components. Observations of the annual average (1998-2000) distribution of total, convective and stratiform precipitation between 20 S to 20N from TRMM suggest that the ratio of convective to stratiform precipitation is > 5 over most land areas and is < 4 over the oceans, with an average value of 4 overall (Schumacher and Houze 2003). However, the stratiform precipitation in Schumaher and Houze refers to deeper cloud systems associated with deep convective clouds and is not directly comparable to model fields that also include warm stratus precipitation. Analysis of precipitation fields from both models for Exp CON (PD), shown in Fig. 4, indicates that although the total precipitation fields are comparable for both models, the GISS model does not capture convective rainfall rates greater than 1.5 m/yr over the Amazon and central Africa as seen in the CSIRO model and in the TRMM analysis. The stratiform precipitation fields between the models differ more significantly with higher values simulated by GISS over the continents (Asia, Central Africa and the Amazon). It appears that the CSIRO model underestimates stratus precipitation over the continents and the GISS model underestimates the convective precipitation over the continents and these differences compensate for small differences in the total precipitation field seen between the two models.

The main difference between the two models is the change in the sign of the LWP differences. This may be related to the treatment of cumulus and stratus coupling. In CSIRO, both the stratus and convective components of LWP increase. The convective LWP is calculated from the same liquid water contents that are saved for the radiation, i.e., from the average of the values before and after the calculation of precipitation. Non-precipitating condensate is detrained only if it reaches the cloud top. Detrained condensate at cloud top is usually small and is typically less than 0.05 g m^{-3} in the grid-box mean. For GISS, LWP decrease is mainly seen in convective clouds. The moist convective LWP is calculated as the integral of liquid water (fraction remaining after removal of the detrained component, condensate that evaporates in the downdraft and precipitation) over the convective plume. The detrained fraction of condensate contributes to the LWP of stratus clouds and not of moist convective clouds. The detrainment of condensate into anvils takes place at each level where condensate exceeds precipitation, and the fraction detrained is larger than that of the CSIRO model. Figure 5 shows global scale distributions of maximum detrained condensate (occurs at 850 hPa as shown in Fig. 6) for both PD and PI aerosol emissions for Exp CON. This difference in the treatment of convective condensate and differences in the detrained fraction may partly explain the difference in sign we obtain for LWP changes between the two models. Thus, the total water path increases in the CSIRO GCM, whereas in the GISS GCM, the reduced total water path is mainly due to the reduction in moist convective LWP (ice water paths (IWP) increase by 0.12). However, since we do not allow for aerosol-ice nuclei interactions nor modify cold cloud precipitation, IWP differences are mainly a response to changes in warm cloud precipitation and the level at which detrainment takes place.

The choice for detrainment depends on cumulus updraft speeds used in the model and terminal vertical velocities of particles, if these can be specified realistically. Problems in large-scale models to adequately resolve cumulus-scale updrafts will result in additional uncertainty when accounting for detrainment effects (DG05). Typically, most models assume that anvil coverage is proportional to convective condensate from updrafts that detrain into the environment (usually a fixed fraction). The CSIRO GCM does not include an explicit parameterization of convective anvils. Instead, condensed detrainment at cloud top increases available moisture for stratus cloud

formation if the relative humidity is above the threshold for cloud formation (85% over oceans and 75% over land). If the relative humidity is below the threshold, the statistical cloud scheme (Smith 1990) instantly evaporates the detrained water. In the GISS GCM convective condensate that gets converted to precipitation follows the treatment described in DG05 (based on Marshall-Palmer droplet distribution), except for warm (liquid-phase) clouds, where the condensate converted to precipitation is based on a droplet threshold size of 14 μm (as described in Sec. 2) and the remainder of condensate in each layer gets detrained. Thus, for polluted conditions, anvil coverage should increase, which although not explicitly calculated, can be extrapolated from the amount of detrained condensate shown in Fig.5. Figure 6 indicates the global annual average values of detrained condensate (liquid + ice) at various levels for Exp CON for both PD and PI aerosol emissions for the GISS GCM. As shown in Fig. 6, the maximum detrainment of condensate takes place at levels where the warm moist convective N_c differences are large. Increased detrainment for PD conditions in the tropical areas (especially over the oceans) as seen in Fig. 5 suggests that these regions may be more susceptible to the aerosol influence.

In terms of radiative effects obtained, both models show an increase in the total water cloud optical depth (15% and 1%, respectively for CSIRO and GISS). However, the optical depths are calculated differently. For CSIRO, total cloud optical depth in each grid box is calculated from the mean in-cloud N_c and LWP (the means being weighted by the stratiform and convective cloud fractions). In both stratiform and convective clouds, the LWP at each time step is taken as the average of the values saved before and after the calculation of precipitation. In the GISS GCM, moist convective cloud optical depth is either a function of droplet size and LWP (function of detrained mixing ratio) for the detrained portion, or is specified as a function of layer thickness for the in-cloud portion (DG05). Thus, increasing aerosols increases moist convective cloud optical depth for the detrained portion. Stratus cloud optical depth is a function of droplet size and LWP. The mean optical depth for stratus and convective clouds are weighted by the respective cloud fractions, similar to CSIRO. The total optical depth in the GISS GCM is then based on the maximum value of optical depth obtained for stratus or convective clouds (Del Genio et al. 1996). The larger percentage increase in total water cloud optical depth (15%) and cloud cover (1.7%) for CSIRO results in more negative values of net CRF (10%). For GISS, the small increase in total water cloud optical depth and cloud cover (~1% for both) result in the 0.2% change in the net CRF. Thus, radiative effects from changes to cumulus precipitation are much higher in the CSIRO GCM than in the GISS GCM.

3.2. Sensitivity of cumulus clouds to cloud droplet number: Differences in N_c between the two models may results in different responses of LWP and radiation to implied aerosol perturbations. To minimize and isolate differences due to aerosols, (since it is much more difficult to employ the same model physics schemes for detrainment effects) we conduct sensitivity tests to evaluate the changes in cloud microphysics, precipitation and radiation due to fixed N_c. Both models used a prescribed distribution based on results from the CSIRO model (values of N_c at 700 hPa from CSIRO (Fig.3) were used to generate uniform vertical profiles of N_c for both PD and PI, separately) to eliminate differences that may arise due to differences in aerosol burdens (Exp CON_C). Differences between Exp CON_C and Exp CON for PD and PI aerosol emissions are shown in Table 2. Although values of N_c at 760 hPa are higher for Exp CON than CON_C for GISS, average column values of N_c are higher in Exp CON_C. N_c values

that influence precipitation are prescribed similarly in both models, however, the treatment of condensate detrainment and its effects on optical depths are different in the two models as discussed earlier. In CSIRO this results in an increase in total LWP (13%) and hence reduces the net CRF (17%), whereas, in the GISS GCM, an overall increase in N_c increases the detrained fraction and reduces the total LWP by a small amount (3%). However, there is no change to the net CRF. A comparison of the results between Exp CON and CON_C indicates that the radiative fluxes in CSIRO are more sensitive to the changes in aerosols and their effects on cloud microphysics, whereas, in GISS, increasing aerosols increases the detrainment and reduces the total LWP. However, the changes are small enough to cause minimal changes in the radiative fluxes. Thus, the radiative effects of aerosols on warm cumulus clouds are much larger in the CSIRO GCM than in GISS. Based on the results obtained from Exp CON and CON_C, the main reason for the differences in radiative fluxes between the two models appears to be related to the treatment of detrained cumulus condensate and its vertical distribution in the GCM, since convective precipitation changes are similar in the two models.

3.3. Effects of aerosols on stratus and cumulus clouds: To evaluate the implications of the changes in LWP and radiation from aerosol suppression of convective precipitation we investigate the influence of anthropogenic aerosols on both stratiform and cumulus warm clouds, (Exp CON_S). We compare changes in cloud properties for differences between PD and PI aerosol emissions for Exp CON and Exp CON_S as shown in Fig. 7 and Table 3. Allowing for the interaction between aerosols and radiation, as well as aerosol effects on stratus clouds, results in more negative values for net TOA radiation and net CRF. As expected, main changes to net TOA radiation, net CRF, cloud cover and LWP come from including aerosol effects on warm stratus clouds. Values of the aerosol indirect effect (net CRF), without aerosol-cumulus cloud interactions, are –0.89 and –1.52 Wm^{-2} for the CSIRO and GISS GCM, respectively (from the difference between Exp CON and CON_S). With aerosol-cumulus cloud interactions, the aerosol indirect effect for the CSIRO and GISS GCM are –2.47 and –1.46 Wm^{-2} respectively.

Accounting for anthropogenic aerosol effects on convective clouds results in shifts in LWPs to lower values (LWP change becomes negative) that are opposite to that obtained when only aerosol effects on stratus clouds are considered for the GISS GCM. A similar study by Menon and Del Genio (2006), using a similar version of the GISS GCM but with different autoconversion and N_c parameterizations, found less negative values of net CRF when including aerosol-cumulus cloud effects. The high value of the aerosol indirect effect usually obtained, from changes to LWP and cloud cover, may thus be lower if suppression of precipitation from aerosol effects on convective clouds are accounted for, at least in the GISS GCM. On the other hand, results from the CSIRO model for Exp CON_S suggests that the addition of aerosol effects on warm cumulus clouds would result in increased LWP and cloud cover, and thus increase the cloud radiative fluxes. Thus, the addition of aerosol effects on both cumulus and stratus clouds can enhance or diminish the net CRF depending on the nature of the LWP changes, which appear to be related to the treatment and distribution of convective condensate and associated anvils.

4. Summary

The effects of aerosols on warm cumulus and large-scale stratiform clouds were investigated

with two climate models, the CSIRO and the GISS GCM. Both models used similar schemes to treat the influence of aerosols on cloud droplet and autoconversion processes. However, the basic model cloud physics and aerosol emissions used in the two models differ considerably. To eliminate differences arising from differences in aerosol concentrations, a sensitivity test was conducted, wherein both models use similar N_c distributions. The changes to condensate distribution, imposed via the influence of aerosols, into precipitation and anvils, appear to produce opposite tendencies for LWP changes. Model results appear to be more sensitive to the treatment of convective condensate than to the aerosol distribution.

In the CSIRO GCM, the effects of detraining condensate only at cloud top and the smaller detrainment rate relative to the GISS GCM result in increasing LWP for both stratus and moist convective clouds, thereby leading to large increases in the total LWP and cloud cover. The radiative fluxes thus decrease with increasing aerosols. In the GISS GCM, the moist convective LWP and precipitation decrease with increasing aerosols. The suppression of precipitation in deep convective clouds due to an increase in aerosols was found to increase the detrainment of cloud water that in turn increases the liquid water in stratus clouds and hence stratus precipitation. Although the GISS GCM neglects the suppression of precipitation from aerosol effects on shallow convective systems, this should not have much of an effect on LWP or precipitation changes due to the underestimation of shallow convection over continents where aerosol changes are larger. The total LWP decreases with increasing aerosols. However, the changes are rather small and the overall influence on radiative fluxes are minimal. The above features, seen in the GISS GCM, are different from the CSIRO GCM perhaps due to the detrainment of non-precipitating condensate to anvils that is allowed to occur at each model level. The end result is that including the effects of aerosols on warm cumulus clouds lowers the large value of the aerosol indirect effect usually obtained from the increase in LWP and cloud cover, at least for the GISS GCM.

Results from the two models suggest that model physics appear to have a more profound influence on LWP changes than do the aerosol distributions. Speculating on the physical nature of responses and model physics used to treat cumulus condensate detrainment are at best exploratory, in the absence of measurements that can address the problem of obtaining the right cumulus scale updraft profiles and the partioning of detrained condensate at appropriate levels in large scale models (DG05). Clearly, the treatment of autoconversion is extremely important since these schemes ultimately affect LWP and precipitation. Within the context of simulations performed with the two GCMs, it appears that the sensitivity of radiation to aerosol effects on warm stratus and cumulus clouds is dependent more on the treatment of cloud condensate than to changes in aerosol or N_c distributions. These results are dependent on the model physics used. Thus, the radiative influence of aerosol effects on warm clouds will remain unconstrained or model dependent without observations of aerosols and its effects on convection and associated anvils. Changes to ice water distribution and the implied radiative effects due to aerosols have not been considered in this paper and will be considered in future work. Future field campaigns such as the Tropical Warm Pool International Cloud Experiment (TWP-ICE) study, being planned in early 2006 in Northern Australia, that plan to examine tropical cirrus and associated convection, may be able to elaborate more on the treatment of convective condensate.

Appendix A:

The CSIRO model includes anthropogenic emissions of sulfur dioxide (Smith et al. 2001) and carbonaceous aerosols (Ito and Penner 2005), both for the year 2000. The carbonaceous aerosol emissions include primary sources of BC and particulate organic matter (POM) from the burning of fossil fuel, open vegetation and biofuel. Since secondary sources of POM were not considered by Ito and Penner, the fossil-fuel POM source for each year was multiplied by 11.2, so that the global emission for 1985 matched that from Liousse et al. (1996), as used in the model intercomparison by Penner et al. (2001). The total anthropogenic aerosol burden for the year 2000 in the CSIRO model are 1.18 TgS as sulfate, 1.18 TgC as OC, and 0.17 TgC as BC. The CSIRO model also includes natural sources of sulfur (Rotstayn and Lohmann 2002) and natural organic carbon from terpenes (Guenther et al. 1995), with a yield of 13% assumed for rapid conversion of terpenes to POM. In addition, number concentrations of two modes of sea salt aerosol (film-drop and jet-drop) are diagnosed as a function of 10-metre wind speed above the ocean surface, following O'Dowd et al. (1997). Sea salt aerosols are assumed to be well mixed in the marine boundary layer, and are set to zero above the top of the boundary layer. Aerosol emissions in the GISS model are specified by the AEROCOM project (An aerosol model intercomparison project: http://nansen.ipsl.jussieu.fr/AEROCOM/aerocomhome.html) and are described in Menon and Del Genio (2006). The total anthropogenic aerosol burden for the year 2000 in the GISS model are 0.86 TgS as sulfate, 0.87 TgC as OC and 0.18 TgC as BC. Although the industrial SO_2 emissions have been increased, the relatively low values of sulfate compared to CSIRO are due to less aqueous phase sulfate production (Koch et al. 2003).

The conversion of aerosol mass to aerosol number, used for the cloud droplet number prediction, is described as follows: For tropospheric sulfate, the size distribution (effective radii=0.05 μm, standard deviation=1.9, density=1.77 g cm^{-3}) follows the fossil-fuel size distribution given in Penner et al. (2001). For carbonaceous aerosols--organic matter (1.3xOC) and black carbon--the size distribution for an internal mixture (effective radii=0.08 μm, standard deviation=1.65, density=1.25 and 1.5 g cm^{-3}, for the mixture and for BC, respectively) follows the biomass burning size distribution given in Penner et al. (2001). For sea salt distributions, the aerosol number used in the CSIRO GCM is as described earlier. In the GISS GCM sea salt mass in the 0.1 to1.0 μm range is converted to an aerosol number following Lohmann et al. (1999) (volume radii=0.44 μm, and density=2.169 g cm^{-3}).

Acknowledgements: The authors gratefully acknowledge Anthony Del Genio of NASA GISS for helpful advice and generous discussions and Danny Rosenfeld for advice in treating aerosol effects on convective clouds based on his observations. This work was funded in part by the Australian Greenhouse Office (LR). We also acknowledge support from the NASA GWEC and NASA Climate Modeling program managed by Don Anderson/Tsengdar Lee, the DOE ARM program and LBNL's LDRD program (SM). The authors thank Kim Nguyen of CSIRO for her careful editing of the manuscript. We also thank Mao-Sung Yao at NASA GISS for help with the GISS GCM.

References

Andreae MO, Rosenfeld D, Artaxo P, Costa AA, Franck GP, Longo KM, Silva-Dias MAF (2004) Smoking rain clouds over the Amazon. Science 303: 1337-1342.

Cooke WF, Wilson JJN (1996) A global black carbon aerosol model. J Geophys Res 101: 19395–19409.

Costa AA, Rosenfeld D, Andreae MO, da Silva Dias MAF, Artaxo P, et al. (2005) LBA-SMOCC-EMFIN:Observations of interactions between aerosols and cloud microphysics over the Amazon. J Geophys Res: (In Review).

Del Genio AD, Kovari W, Yao MS, Jonas J (2005) Cumulus microphysics and climate sensitivity. J Clim 18: 2376-2387.

Del Genio AD, Yao MS (1993) Efficient cumulus parameterization for long-term climate studies: The GISS scheme. In The representation of cumulus convection in numerical models (K.A. Emanuel and D.A. Raymond, Eds.) Vol. 24, no. 46. AMS Meteor. Monograph pp. 181-184. Amer Meteorol Soc.

Del Genio AD, Yao MS, Lo KKW (1996) A prognostic cloud water parameterization for global climate models. J Clim 9: 270-304.

Ghan SJ, Easter RC, Chapman E, Abdul-Razaak H, Zhang Y, Leung R, Laulainen N, Saylor R, Zaveri R (2001) A physically-based estimate of radiative forcing by anthropogenic sulfate aerosol. J Geophys Res 106: 5279-5293.

Gordon HB, Rotstayn LD, McGregor JL, Dix MR, Kowalczyk EA, O'Farrell SP, Waterman LJ, Hirst AC, Wilson SG, Collier MA, Watterson IG, Elliott TI (2002) The CSIRO Mk3 Climate System Model. CSIRO Atmospheric Research technical paper no. 60, Aspendale, Australia. 130 pp.

Graf HF (2004) The complex interaction of aerosols and clouds. Science 303: 1309-1311.

Gregory D, Rowntree PR (1990) A mass flux convection scheme with representation of cloud ensemble characteristics and stability-dependent closure. Mon Weather Rev 118: 1483-1506.

Guenther A, Hewitt CN, Erickson, Fall R, Geron C, Graedel T, Harley P, Klinger L, Lerdau M, McKay WA, Pierce T, Scholes B, Steinbrecher R, Tallamraju R, Taylor T, Zimmerman P (1995) A global model of natural volatile organic compound emissions. J Geophys Res 100: 8873-889

Gultepe I, Isaac GA (1999) Scale effects on averaging of cloud droplet and aerosols number concentrations: Observations and models. J Clim 12: 1268-1279.

Hansen JE, Sato Mki, Ruedy R, Nazarenko L, Lacis A et al. (2005) Efficacy of climate forcings. J Geophys Res 110:doi:10.1029/2005JD005776.

Ito A, Penner JE (2005) Historical emissions of carbonaceous aerosols from biomass and fossil fuel burning for the period 1870-2000. Glob Biogeochem Cyc In press.

Koch D, Park J, Del Genio A (2003) Clouds and sulfates are anticorrelated: A new diagnostic for global sulfur models. J Geophys Res 108: doi: 101029/2003JD003621.

Liousse C, Penner JE, Chuang C, Walton JJ, Eddleman H, Cachier H (1996) A global three-dimensional model study of carbonaceous aerosols. J Geophys Res 101: 19411-19432.

Liu YG, Daum PH (2000) Spectral dispersion of cloud droplet size distributions and the parameterization of cloud droplet effective radius. Geophys Res Lettr 27:1903-1906.

Lohmann U, Feichter J, Chuang CC, Penner JE (1999) Predicting the number of cloud droplets in the ECHAM GCM. J Geophys Res 104: 9169-9198.

Lohmann U, Feichter J (2005) Global indirect aerosol effects: a review. Atmos Chem Phys 5: 715-737.

Menon S, Del Genio AD (2006) Evaluating the impacts of carbonaceous aerosols on clouds and climate. To appear in "Human-induced climate change: An interdisciplinary Assessment", Edited by Schlesinger et al. Cambridge University Press.

Menon S (2004) Current uncertainties in aerosol climate effects. Ann Rev 29:1-30.

Menon S, Del Genio AD, Koch D, Tselioudis G (2002) GCM simulations of the aerosol indirect effect: Sensitivity to cloud parameterization and aerosol burden. J Atmos Sci 59: 692-713.

Menon S, Brenguier JL, Boucher O, Davison P, Del Genio AD, et al. (2003) Evaluating Cloud-Aerosol Process Parameterizations with Single Column Models and ACE-2 Cloudy Column Observations. J Geophys Res 108: doi:10.1029/2003JD003902

Nober FJ, Graf HF, Rosenfeld D (2003) Sensitivity of the global circulation to the suppression of precipitation by anthropogenic aerosols. Glob Planetary Change 37: 57-80.

O'Dowd CD, Smith MH, Consterdine IE, Lowe JA (1997) Marine aerosol, sea-salt, and the marine sulphur cycle: a short review. Atmos Environ 31: 73-80.

Penner JE, Andreae M, Annegarn H, Barrie L, Feichter J, Hegg D, Jayaraman A, Leaitch R, Murphy D, Nganga J, Pitari G (2001) Aerosols, their direct and indirect effects. In Climate Change 2001: The Scientific Basis, edited by J. T. Houghton et al., Cambridge Univ. Press. 289-348.

Ramanathan V, Collins W (1991) Thermodynamic regulation of ocean warming by cirrus clouds deduced from observations of the 1987 El Nino. Nature 351: 27-32.

Rosenfeld D (2000) Suppression of Rain and Snow by Urban and Industrial Air Pollution. Science 287: 1793-1796.

Rosenfeld D, Lensky IM (1998) Satellite-based insights into precipitation formation processes in continental and maritime convective clouds. Bull Amer Meteorol Soc 79: 2457-2476.

Rosenfeld D, Woodley WL (2000) Deep convective clouds with sustained supercooled liquid water down to –37.5C. Nature 405: 440-442.

Rosenfeld D (1999) TRMM observed first direct evidence of smoke from forest fires inhibiting rainfall. Geophys Res Lettr 26: 3105-3108.

Rotstayn LD (1997) A physically based scheme for the treatment of stratiform clouds and precipitation in large-scale models, 1, Description and evaluation of the microphysical processes. Quart J Roy Meteor Soc 123: 1227-1282.

Rotstayn LD (2000) On the "tuning" of autoconversion parameterizations in climate models. J Geophys Res 105: 15495-15507.

Rotstayn LD, Lohmann U (2002a) Tropical rainfall trends and the indirect aerosol effect. J Climate 15: 2103-2116.

Rotstayn LD, Lohmann U (2002b) Simulation of the tropospheric sulfur cycle in a global model with a physically based cloud scheme. J Geophys Res 107: doi:10.1029/2002JD002128.

Rotstayn LD, Liu Y (2003) Sensitivity of the first indirect aerosol effect to an increase of cloud droplet spectral dispersion with droplet number concentration. J Climate 16: 3476-3481

Rotstayn LD, Liu YG (2005) A smaller global estimate of the second indirect aerosol effect. Geophys Res Lettr 32: doi:10.1029/2004GL021922.

Rotstayn LD (1999) Indirect forcing by anthropogenic aerosols: A global climate model calculation of the effective-radius and cloud-lifetime effects. J Geophys Res 104: 9369-9380.

Schumacher C, Houze RA Jr. (2003) Stratiform rain in the tropics as seen by the TRMM precipitation radar. J Clim 16: 1739-1756.

Segal Y, Khain A, Pinsky M, Sterkin A (2004) Sensitivity of raindrop formation in ascending cloud parcels to cloud condensation nuclei and thermodynamic conditions. Q J R Meteorol

Soc 130: 561-581.
Shepherd MJ, Oierce H, Negri AJ (2001) Rainfall modification by major urban areas: observations from spaceborne rain radar on the TRMM satellite. J Appl Meteorol 41: 689-701.
Smith RNB (1990) A scheme for predicting layer clouds and their water content in a general circulation model. Quart J Roy Meteor Soc 116: 435–460
Smith SJ, Pitcher H, Wigley TML (2001) Global and regional anthropogenic sulfur dioxide emissions. Global Planetary Change 29: 99-119.
Takemura T, Nozawa T, Emori TS, Nakajima TY, Nakajima T (2005) Simulation of climate response to aerosol direct and indirect effects with aerosol transport-radiation model. J Geophys Res 110: doi:101029/2004JD00502.

Table 1: Description of microphysical processes used in the models for the various simulations. The cloud droplet number concentration (N_c) from the aerosol concentration N_{al} and N_{ao} (land and ocean, respectively) for cumulus (C) and large-scale stratus clouds (S) is as given. The autoconversion treatment is based on a modified version of the treatment used in Rotstayn and Liu (2005) (RL05) for S.

Simulation	N_c (cm^{-3})		Autoconversion	
	C	S	C	S
Exp CON	$174.8+1.51N_{al}^{0.886}$ $-29.6+4.92N_{ao}^{0.694}$	Land: 200 Ocean: 50	Based on a droplet threshold size of 14 μm.	RL05
Exp CON_S	Same as above	$-595 + 298 \log N_{al}$ $-273 + 162 \log N_{ao}$	Same as above	RL05

Table 2: Annual average differences between present-day (PD) and pre-industrial (PI) aerosol emissions for CSIRO and GISS GCM for Exp CON and CON_C. S and C stand for stratus and cumulus, respectively. τ_c refers to total optical depth for water clouds. GISS values for N_c are at 760 hPa.

Variable	CSIRO		GISS	
	CON	CON_C	CON	CON_C
TOA Net radiation (W m^{-2})	-1.31	-2.12	0.02	0.08
Net CRF (W m^{-2})	-1.58	-2.43	0.06	0.00
Total cloud (%)	1.08	1.40	0.05	-0.03
Convective cld (%)	1.38	2.24	-0.01	-0.03
Water τ_c	0.92	1.34	0.14	0.27
LWP (g m^{-2})	1.44 (S)	2.25 (S)	-0.07 (S)	0.1 (S)
	5.03(C)	7.49 (C)	-1.03 (C)	-1.66 (C)
Total LWP	6.47	9.74	-1.14	-1.55
IWP (g m^{-2})	1.77 (S)	2.89 (S)	0.01 (S)	-0.11 (S)
	0.69 (C)	1.20 (C)	0.11(C)	0 (C)
Total IWP	2.46	4.09	0.12	-0.11
Total Precip. (mm/d)	-0.025	-0.019	0.0	-0.002
Convective Precip. (mm/d)	-0.051	-0.072	-0.041	-0.07
N_c (cm^{-3}) @700 hPa	75	75	118	66
Aerosol burden (mg m^{-2})	5.67	5.67	4.45	4.45

Table 3: Similar to Table 2 but differences are for Exp CON and CON_S.

Variable	CSIRO		GISS	
	CON	CON_S	CON	CON_S
TOA Net radiation (W m^{-2})	-1.31	-3.41	0.02	-2.41
Net CRF (W m^{-2})	-1.58	-2.47	0.06	-1.46
Total cloud (%)	1.08	1.47	0.05	0.35
Convective cloud (%)	1.38	1.50	-0.01	0.05
Low cloud (%)	0.54	0.97	0.02	0.45
Water $\square_c$	0.92	1.50	0.14	3.14
LWP (g m^{-2})	1.44 (S)	3.32 (S)	-0.07 (S)	1.56 (S)
	5.03(C)	5.24 (C)	-1.03 (C)	-0.85(C)
Total LWP	6.47	8.56	-1.14	0.71
IWP (g m^{-2})	1.77 (S)	1.70 (S)	0.01 (S)	0.65(S)
	0.69 (C)	0.69 (C)	0.11(C)	0.04(C)
Total IWP	2.46	2.39	0.12	0.69
Total Precip. (mm/d)	-0.025	-0.022	0.00	-0.012
Convective Precip. (mm/d)	-0.051	-0.048	-0.042	-0.035

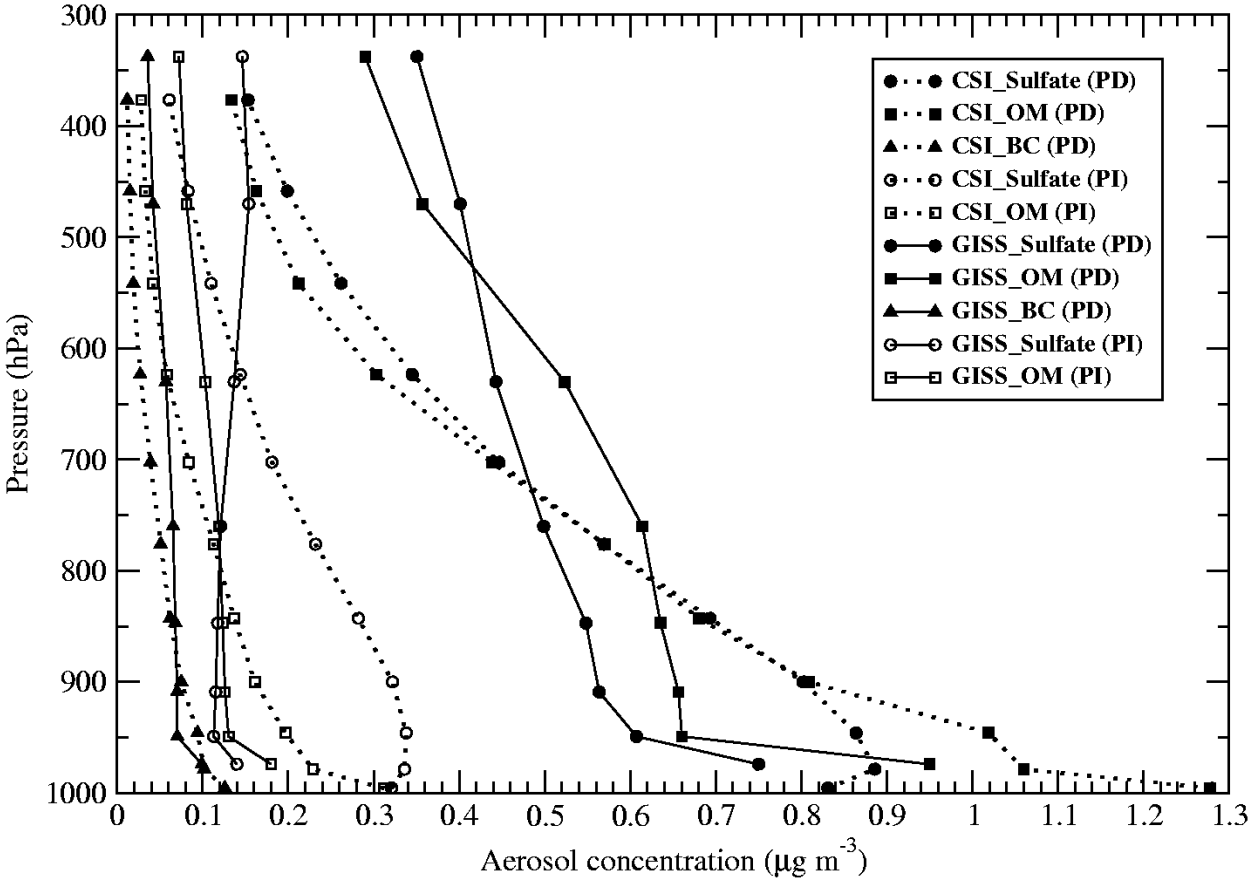

Figure 1: Vertical profile of global annual average values of aerosol concentration for Exp CON for present day (PD) and pre-industrial (PI) aerosol emissions for sulfate, organic matter (OM), and black carbon (BC). BC values for PI are usually very low (<< 0.1 □g m^{-3}) and are not shown as are values at levels less than 300 hPa.

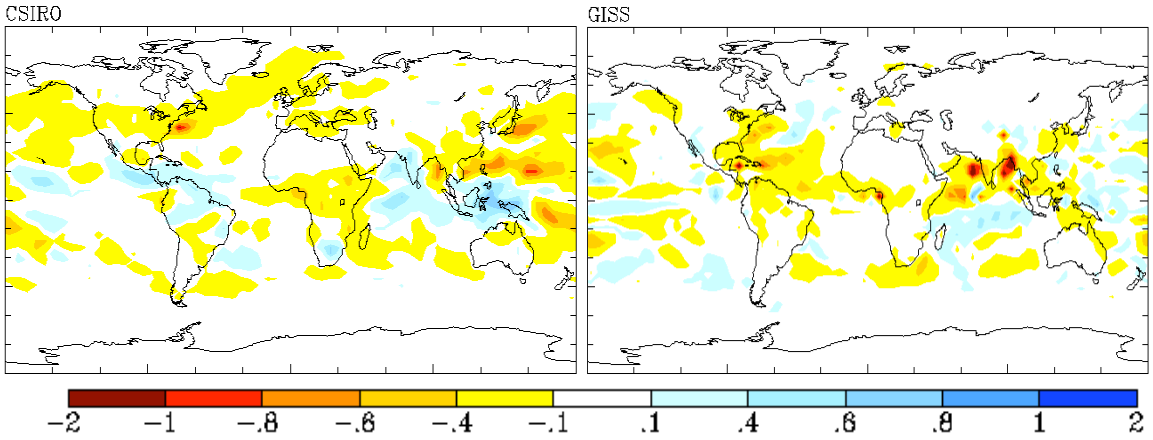

Figure 2: Global annual differences in convective cloud precipitation (mm/day) between present day and pre-industrial aerosol emissions for CSIRO and GISS for Exp CON.

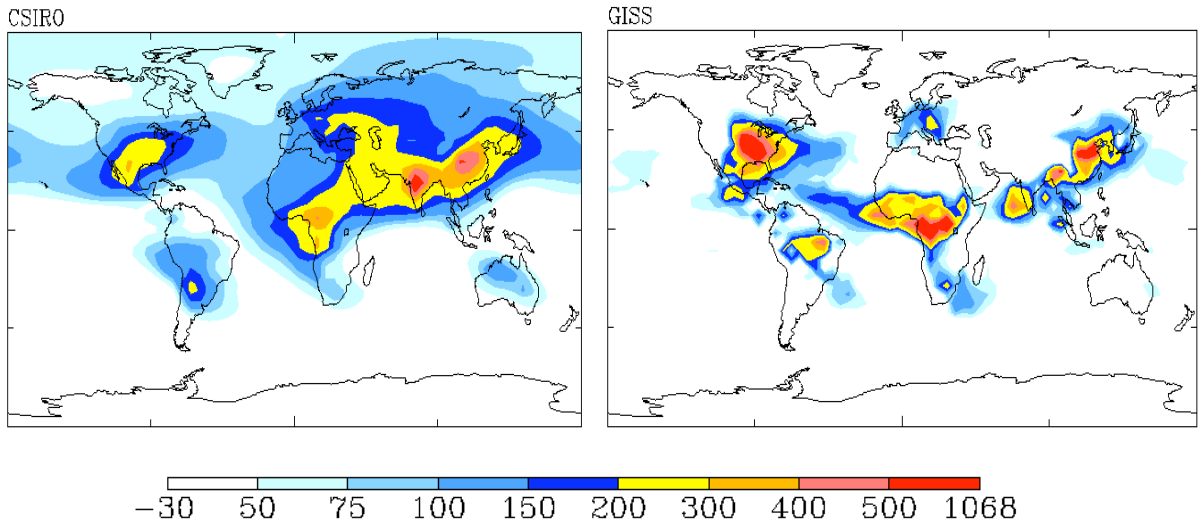

Figure 3: Global annual differences in cloud droplet number concentration (N_c) (cm^{-3}) between present day and pre-industrial aerosol emissions for warm moist convective clouds for Exp CON for CSIRO and GISS at 700 and 760 hPa, respectively.

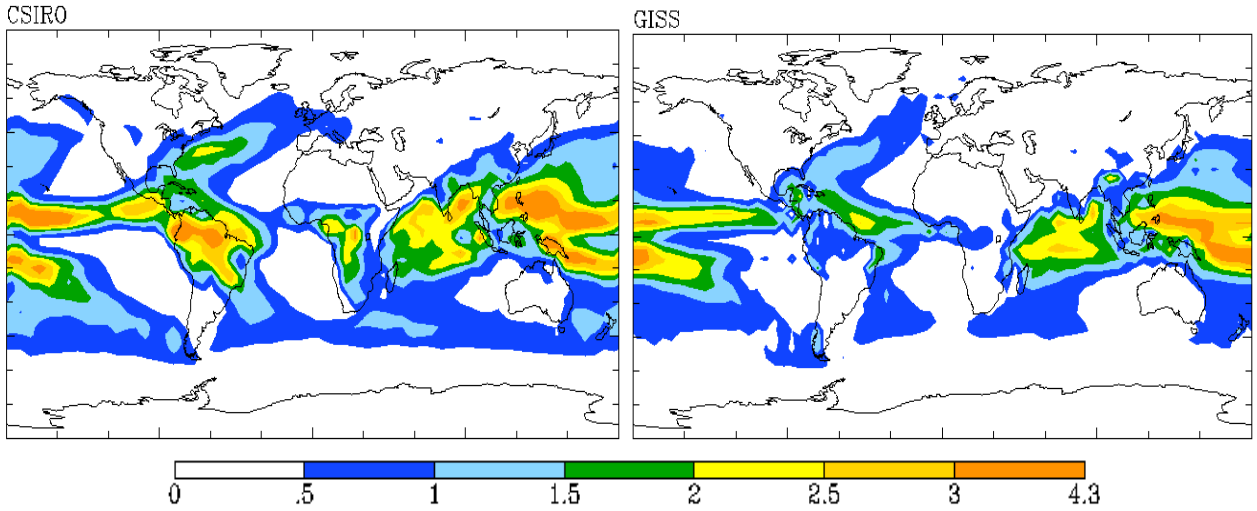

Figure 4: Global annual convective cloud precipitation (m/yr) for present day aerosol emissions for CSIRO and GISS for Exp CON. Units are chosen to facilitate comparison with TRMM data (Fig. 3 of *Schumacher and Houze* 2003).

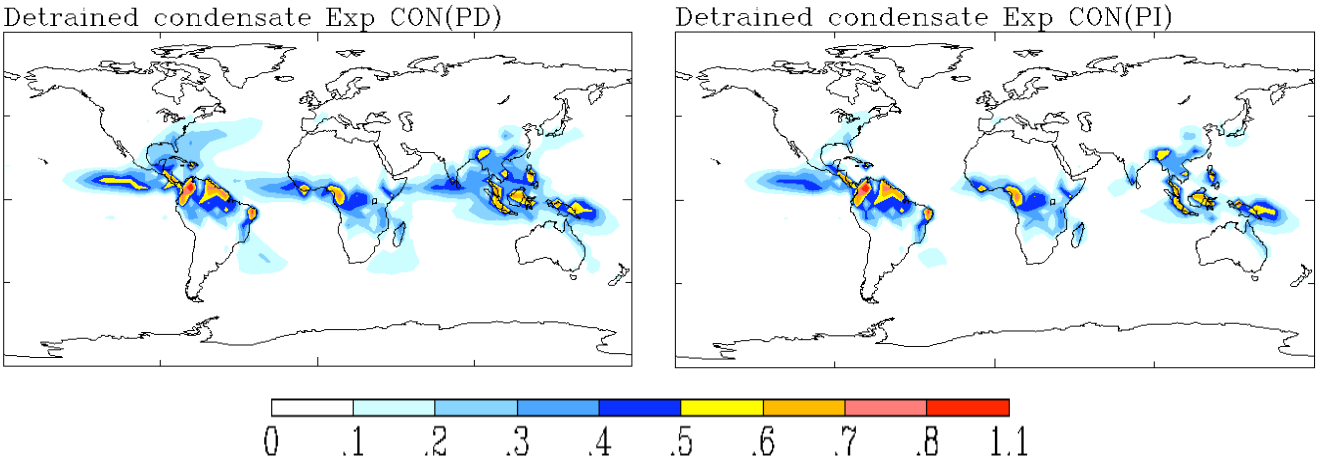

Figure 5: Global annual average values of detrained condensate (g m^{-3}) for Exp CON for present day (PD) and pre-industrial (PI) aerosol emissions at 850 hPa (level of maximum detrainment) for GISS.

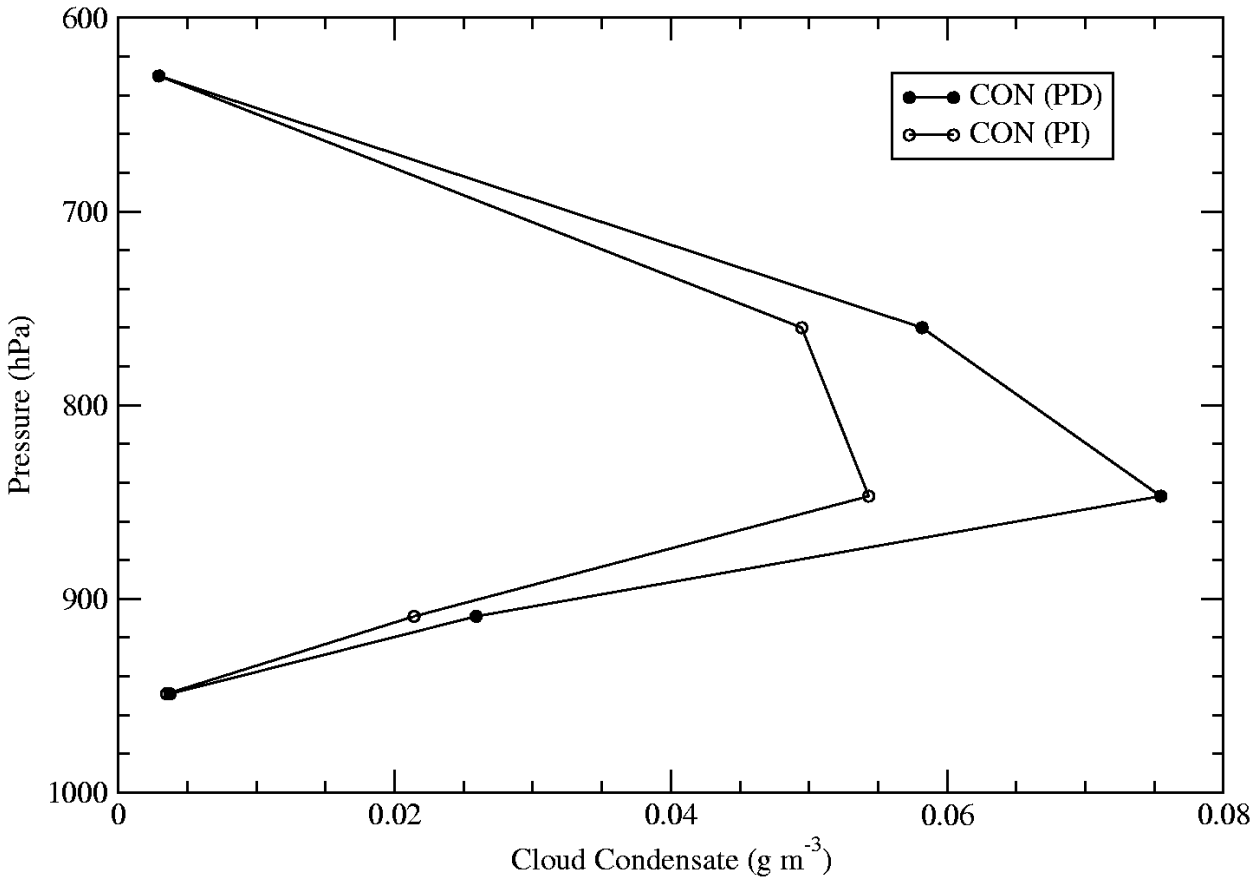

Figure 6: Vertical profile of global annual average values of detrained cloud condensate (g m^{-3}) for Exp CON for both present day (PD) and pre-industrial (PI) aerosol emissions for GISS.

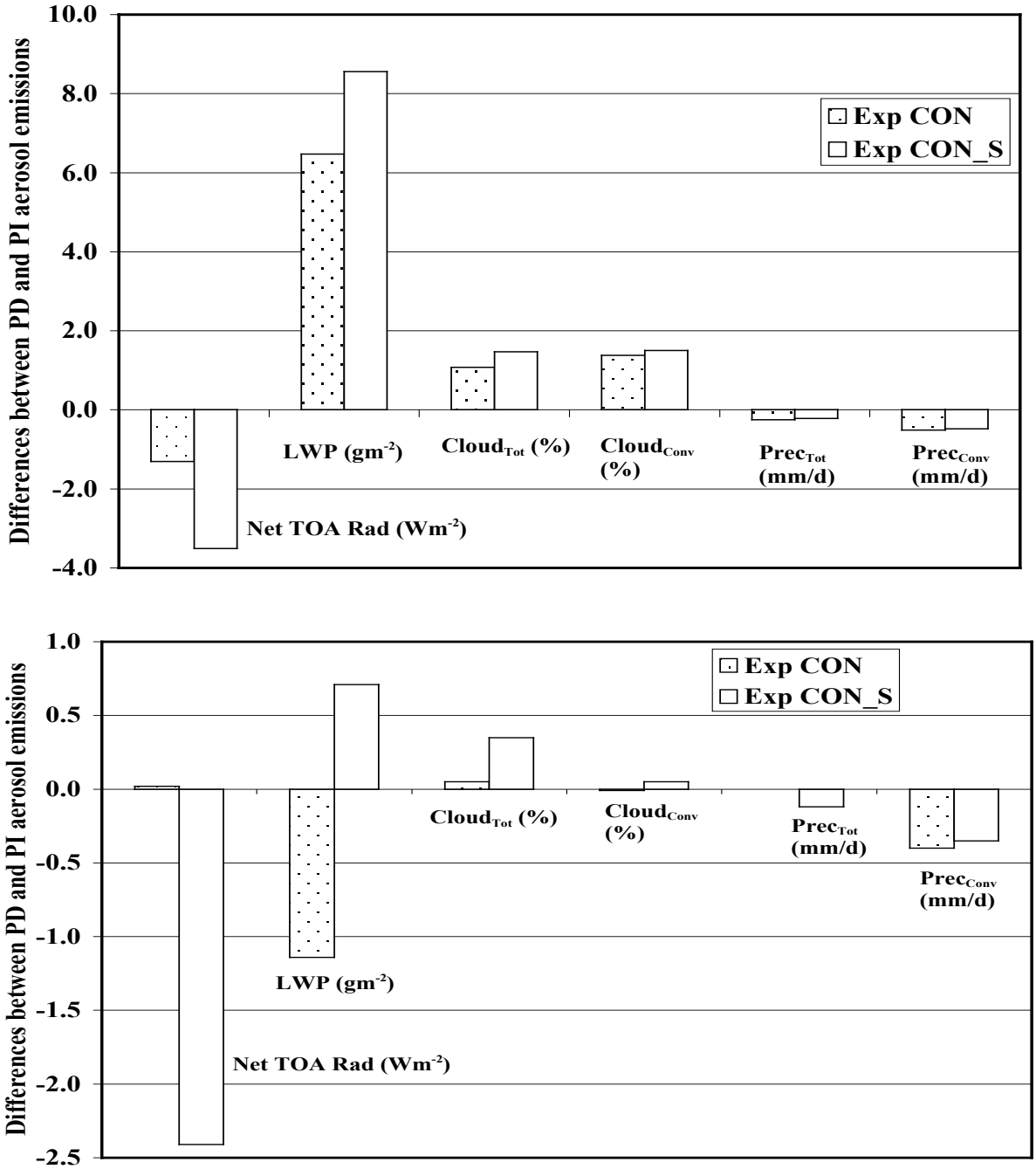

Figure 7: Differences between present-day (PD) and pre-industrial (PI) aerosol emissions for various diagnostics for Exp CON and CON_S for the CSIRO (top) and GISS (bottom) GCM. Differences are based on global annual averages. Note that precipitation changes are scaled by a factor of 10.